Hindawi
Shock and Vibration
Volume 2021, Article ID 6643894, 8 pages
https://doi.org/10.1155/2021/6643894

Research Article

A Simulation Study on the Spatial-Temporal Characteristics of Pore Water Pressure and Roof Water Inrush in an Aquiclude

Tao Yang,[1,2] Ji Li,[1,2] Longwen Wan,[3] and Sheng Wang[3]

[1]*Xi'an University of Science and Technology, Xi'an, Shaanxi 710054, China*
[2]*Key Laboratory of Western Mine Exploitation and Hazard Prevention with Ministry of Education, Xi'an University of Science and Technology, Xi'an 710054, China*
[3]*Longmenxia South Coal Mine of Sichuan Huayingshan Coal Industry Co., Ltd., Guang'an 638020, China*

Correspondence should be addressed to Ji Li; liji@xust.edu.cn

Received 17 December 2020; Revised 24 January 2021; Accepted 2 February 2021; Published 15 February 2021

Academic Editor: Feng Du

As the working face advances, the overlying aquiclude is subjected to periodic dynamic loads, causing pore water pressure distortion, which provides important forewarning for a water inrush disaster in shallow coal seams. In order to analyze the pore water pressure in an aquiclude and determine the spatial-temporal characteristics of the water inrush, the aquiclude is simplified into a saturated, porous, liquid-solid medium and a viscoelastic dynamic model is created to obtain the analytical solution of the pressure distribution. FLAC3D is used to develop a fluid-solid coupling model and to analyze the characteristics of the pressure change and overburden under different mining intensities. This study on pore water pressure in an aquiclude and the determination of the spatial-temporal characteristics of the water inrush provides a foundation for developing early-warning systems for roof water inrush.

1. Introduction

In recent years, the coal exploitation intensity has increased in the western coal mining areas in China and exploitations under thin bedrock and in water-rich areas have caused frequent occurrences of coal mining water inrush [1, 2]. In the coal mining areas in the northern areas of Shaanxi province, the coal stockpiles are stable and abundant and suitable for exploitation with high-intensity mechanized mining equipment. However, the coal seams in the northern area of Shaanxi province are shallow and as a result, the unique and critical aquiclude easily becomes unstable [3] because of the strong mining disturbance and water seepage. Furthermore, the instability makes the areas prone to large-scale flooding disasters and also affects the environmentally friendly development of coal mines [4]. Thus, it is necessary and essential to pay more attention to the potential danger of water inrush due to mining disturbance and to examine carefully the reasons for the roof water inrush and the required precautions in these mining areas [5–7] and take into account the vulnerable ecosystems and high-intensity exploitation.

Many scholars have focused on the mechanism of and safeguards against roof water inrush [8–11]. Gao developed the "Four-Zone" model of rock movement based on the "Three-Zone" model [12]. According to Gao, a mechanical model of the rock formation should be divided into the rupture zone, abscission zone, sagging zone, and loose impingement zone. This research develops new thoughts for the subsequent exploration of roof water inrush. Shi et al. [13] derived an equation of the water flow in the fractured zone with multiple factors from the "Four-Zone" model and validated its applicability. Wu et al. [14] designed a three-dimensional visual model of water inrush from a coal seam roof and implemented a dynamic simulation of the bedrock cracking and groundwater flow field using visualization in the foundation of the "Three Maps" method. Fan et al. [15] identified the critical factors influencing water and sand inrush in the Yushenfu coal mine, and these factors included the sand thickness, aquiclude water richness, the thickness of the

effective water-resistant layer, and the area of mining disturbance. Subsequently, they established an assessment model of water and sand inrush and conducted an integrated analysis of the threat of water and sand inrush in the Yushenfu coal mine. Wang and Han [16] established a flood monitoring and forecasting system based on the aquiclude water level and water quality. Sui and Dong [17] found that pore water pressure is an important indicator for monitoring and forecasting quicksand hazards in mines and used a centrifugal model of a mining subsidence experiment. Yang et al. [18] proposed that the essential characteristic of mine water inrush is the rock mass rupture induced by the disturbance due to mining pressure and water pressure in the stress field. It was found that the forecasting research on roof water inrush disasters is not limited to the small area of the surrounding rock and bedrock but has also focused on the dynamic tracking of the fluid migration of the overlying aquicludes, that is, the natural water protection. The aquiclude in the northern area of Shaanxi Province consists of Hipparion laterite from the Tertiary period and its lithology consists of ball clay and sandy loam [19]. Zhang et al. [20] analyzed the supervoid water pressure characteristics of the clay below an area suffering an earthquake and the main factors influencing the changes in the supervoid water pressure using an earthquake-simulating shaking table test. Based on the similarity between the influences of mining disturbances and the transfer of the wave frequency of an earthquake to a periodic dynamic load, we assume that the spatial-temporal characteristics of roof water inrush can be observed by the changes in the pore water pressure in an aquiclude as a result of mining disturbances; in addition, we propose that the "hydraulic pressure-stress" spatial-temporal system can be determined for the "aquiclude coal seam" structure. This study is focused on the determination of the spatial-temporal characteristics of the water inrush using qualitative and quantitative analyses to prevent water inrush disasters from the roof.

2. Methodology

In the northern areas of Shaanxi province, the geological condition of shallow coal seam is quite thin bedrock. In the coal mines, periodic cracking occurs in the overlying roof [21]. Aquicludes possess the features of softness and viscoelasticity and the transient deformation does not synchronize with the lagging deformation of the bedrock; therefore, this is a passive deformation. The periodic impact load of a layer occurs due to the gravity stress of the loose cover and the pressure of the bedrock below. We used the Biot equation [22] of saturated linear elastic porous media to focus on the layer dynamic loading and the viscoelasticity dynamic model put forward by Wei and Muraleetharan [23]. In Figure 1, the aquiclude is simplified into a saturated porous solid-liquid mixture and the viscoelasticity dynamic model of the aquiclude is established. The fluctuations in the layer's pore water pressure are analyzed under the load of periodic stress frequency. The periodic pressure in the working face is a function of time and the coal seam propulsion position is a function of space.

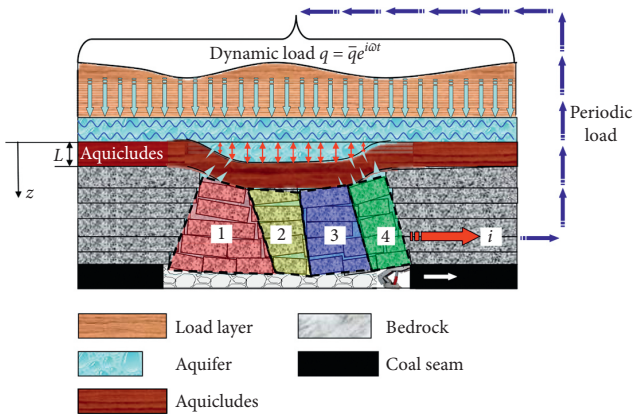

Figure 1: Viscoelasticity dynamic model of a soil layer.

To simplify the three-dimensional problem to a two-dimensional problem, L is the thickness of the aquiclude and the dynamic load q is identified by the following equation:

$$q = \overline{q}e^{i\omega t}, \tag{1}$$

where $\overline{q}$ is the load amplitude, ω is the frequency of the load transfer angle, t refers to time, and i is the transfer time, that is, the frequency of the periodic stress of the working face.

According to the governing equation of saturated porous media under the influence of a dynamic load introduced by Zienkiewicz et al. [24], the solid-liquid mixture per volume represents the object (soil framework and water), $\ddot{u}_i$ is the displacement of the aquiclude framework (solid), and $\ddot{w}$ corresponds to the relative average speed of water (liquid). The governing equation of the soil layer movement is

$$\sigma_{ij} + \rho g_i = \rho \ddot{u}_i + \rho_f \ddot{w}_i, \tag{2}$$

$$\rho = (1-n)\rho_s + n\rho_f, \tag{3}$$

where σ_{ij} refers to the Cauchy stress tensor, ρ_s is the density of the aquiclude framework, ρ_f corresponds to the density of water, and g_i is the gravitational acceleration.

When the pore water of the aquiclude framework is used as the analysis object, the liquid movement equation of the pore fluid per volume is defined as

$$-p + \rho_f g_i = \rho_f \ddot{u}_i + \left(\frac{\rho_f \ddot{w}_i}{n}\right) + \left(\frac{\rho_f g_i \ddot{w}_i}{k}\right), \tag{4}$$

where p is the pore water pressure, n is the pore frequency, and k refers to the permeability coefficient of the aquiclude.

If the elastic damage occurs prior to the damage of the aquiclude, the constitutive relation of the aquiclude is presented in the following equation:

$$\sigma = \left[\left(\widetilde{K}_U - \frac{2}{3}G\right)\nabla \cdot u + \widetilde{\alpha}_B \widetilde{M} \nabla \cdot w\right]1 + G\left[\nabla u + (\nabla u)^T\right], \tag{5}$$

$$-p^w = \widetilde{M}\left(\widetilde{\alpha}_B \nabla \cdot u + \nabla \cdot w\right), \tag{6}$$

where $(1/\widetilde{M}(\varpi)) = (n_0^s/(K_s + n_0^s\Theta_W(1 + i\varpi\tau_w))) + (n_0^w/K_w)$, $\widetilde{\alpha}_B(\varpi) = 1 - (n_0^s[\lambda' + n_0^s\Theta_W(1 + i\varpi\tau_w)]/K_s + n_0^s\Theta_W(1 + i\varpi\tau_w))$, $\widetilde{K}_U(\varpi) = \widetilde{M}\widetilde{\alpha}_B + \widehat{K} + [(n_0^s(K_S - \lambda')^2/K_S) - (n_0^s(K_S$

$-\lambda')^2/K_s + n_0^s\Theta_W(1 + i\omega\tau_w))]$, $\widehat{K} = n_0^s(\lambda_s + (2/3) \quad \mu_s) - (n_0^s(\lambda')^2/K_s)$, where K_W is the bulk modulus of the pore fluid; K_S is the bulk modulus of the solid particles of the soil; λ_S is the lame constant of the soil layer framework; λ' is the coupling modulus between the compression of the soil body and the deformation of the framework; Θ_W is the differential pressure induced by the changes in the voidage volume under static conditions; and τ_w is the time of the local flow features. In this study, it is assumed that the soil layer is an ideal homogeneous medium and the value of τ_w is 0.

The boundary condition of the viscoelasticity dynamic model of the aquiclude is presented in the following equation:

$$\left.\begin{aligned} &\overline{z} = 0, \quad \overline{\sigma} = \overline{q}, \quad \overline{p} = 0, \\ &\overline{z} = 1, \quad \overline{u} = 0, \quad \left(\frac{\mathrm{d}\overline{p}}{\mathrm{d}\overline{z}}\right) = 0. \end{aligned}\right\} \tag{7}$$

By simplifying equation (2) and equation (4), the following equations are deduced:

$$\frac{\mathrm{d}\sigma}{\mathrm{d}z} = \rho\ddot{u} + \rho_f\ddot{w}, \tag{8}$$

$$-\frac{\mathrm{d}\sigma}{\mathrm{d}z} = \rho\ddot{u} + \left(\frac{\rho_f\ddot{w}}{n}\right) + \left(\frac{\rho_f g\ddot{w}}{k}\right). \tag{9}$$

By plugging the constitutive relation equations (5) and (6) into equations (8) and (9), the following governing equation is deduced with the displacement as the variable:

$$\begin{aligned} &\left(\widetilde{K}_U - \frac{2}{3}\widetilde{G} + 2G\right)\frac{\partial^2\overline{u}}{\mathrm{d}\overline{z}^2} + \widetilde{\alpha}_B\widetilde{M}\frac{\partial^2\overline{w}}{\mathrm{d}\overline{z}^2} = -L^2\omega^2\left(\rho\overline{u} + \rho_f\overline{w}\right), \\ &\widetilde{M}\left(\widetilde{\alpha}_B\frac{\partial^2\overline{u}}{\mathrm{d}\overline{z}^2} + \frac{\partial^2\overline{w}}{\mathrm{d}\overline{z}^2}\right) = -L^2\omega^2\rho_f\left(\overline{u} + \frac{\overline{w}}{n}\right) \\ &\qquad + i\omega L^2\rho_f g\frac{\overline{w}}{k}. \end{aligned} \tag{10}$$

In order to ensure consistency in the equations, we suppose that all variables and the frequency of the external load transfer are identical. Subsequently, the boundary condition shown by the principal variable can be obtained:

$$\left.\begin{aligned} &\overline{z} = 0, \quad \left(\widetilde{K}_U + \frac{4}{3}G - \widetilde{\alpha}_B\widetilde{M}\right)\frac{\mathrm{d}\overline{u}}{\mathrm{d}\overline{z}} = \overline{q}L, \\ &\left(\widetilde{K}_U + \frac{4}{3}G - \widetilde{\alpha}_B\widetilde{M}\right)\frac{\mathrm{d}\overline{w}}{\mathrm{d}\overline{z}} = -\widetilde{\alpha}_B\overline{q}L, \\ &\overline{z} = 1, \overline{u} = 0, \overline{w} = 0. \end{aligned}\right\} \tag{11}$$

Thus, the analytic solution of the value of the load amplitude $\overline{p}$ is defined as

$$\overline{p} = \frac{-\widetilde{M}\left[\widetilde{\alpha}_B\sum_{i=1}^{4}c_i\lambda_i\exp(\lambda_i\overline{z}) + \sum_{i=1}^{4}c_{i+4}\lambda_i\exp(\lambda_i\overline{z})\right]}{L}, \tag{12}$$

where λ_i is the characteristic solution of the differential equations; c_i is an undetermined coefficient.

Therefore, we can obtain the amplitude of the water pressure of the aquicludes in real time according to the analytic formula of clay layer's pore water pressure and compare it with the maximum of the water-inrush pressure threshold at the site to describe the dynamic changes in the pore water pressure corresponding to the working face advance.

3. Simulations of the Dynamic Response of the Pore Water Pressure

We established a solid-liquid coupling model and made several assumptions based on the FLAC3D [25–27] percolation module to visually monitor the spatial-temporal behavior of the pore water pressure of the aquicludes during the mining process. The assumptions are as follows: the rock mass and aquicludes are a porous media continuum; the deadweight stress field is also the initial stress field; anhydrous and nonpressurized processing is used for the mined coal mass; saturated, stable, isotropic flow rules are used in the liquid constitutive model. The porosity, osmotic coefficient, and other parameters are those of the geological conditions of the Han Jiawan coal mine in the northern mine area in Shaanxi Province.

3.1. FLAC3D Solid-Liquid Fundamental Coupling Theory. The problems of mining disturbance and seepage that occur during mining are not only related to the rock and soil mechanics and hydraulics but are also affected by the lithology of the overburden rock, its structures, and the geological environment. There are parallels between the liquid flow simulation and the determination of the framework structure when using FLAC3D to simulate the flow of porous media. Subsequently, the isotropic and Model fl_isotropic are applied. The main focus of the computing process is the determination of the changes in the rock mass stress field as a result of the increases or decreases in the pore water pressure. The displacement of the liquid flow is based on Darcy's law and the process of the solid-liquid coupling satisfies the Biot equation. In the simulation, the equivalent continuum mathematical model and the synchronization and rigor are obtained based on the FISH language.

The key equations of the coupling simulation are as follows:

The equilibrium equation:

$$-q_i + q_v = \frac{\partial\zeta}{\partial t}. \tag{13}$$

The vibration equation:

$$q_i = -k\left(p - \rho_f x_j g_i\right). \tag{14}$$

The constitutive relation:

$$\frac{1}{Q}\frac{\partial p}{\partial t} + \frac{n}{s}\frac{\partial s}{\partial t} = \frac{1}{s}\frac{\partial\zeta}{\partial t} - \alpha\frac{\partial\varepsilon}{\partial t} + \beta\frac{\partial T}{\partial t}. \tag{15}$$

The compatible equation:

$$\varepsilon_{ij} = \frac{\left(v_{ij} + v_{ji}\right)}{2}. \tag{16}$$

In the above equations,

$$\frac{\partial \zeta}{\partial t} = \frac{1}{Q}\frac{\partial p}{\partial t} + \alpha\frac{\partial \varepsilon}{\partial t} - \beta\frac{\partial T}{\partial t}, \tag{17}$$

where q_i is the seepage speed; q_v is the fluid source strength of the tested volume; and ζ is the change in the fluid volume of the pore media per volume. Q is the Biot modulus; p is the pore pressure; α is the Biot coefficient; ε is the volume strain; T is the temperature; β is the coefficient of thermal expansion; k is the osmotic coefficient; ρ_f is the fluid density; g_i is the component of gravity acceleration; and v is the velocity at one point.

3.2. Establishment of the FLAC3D Solid-Liquid Coupling. The specific dimensions of the three-dimensional model are 300 m × 300 m × 150 m and it is based on the 2045 working face at the Han Jiawan coal mine. 2-2 coal is exploited from this working face and the thickness of the coal seam ranges from 2.5 m to 5.0 m and the average thickness is 4.3 m [28–30]. The dip angle of the coal seam is 1°–3°. The strike length of the working face is 2700 m and its dip expansion is 220 m. The thickness of the bedrock covering the coal seam ranges from 62 m to 102 m. The thickness of the aquiclude is about 30 m and it lies below a water-rich aquifer. In order to decrease the boundary effect, boundary coal pillars with a height or length of 50 m exist in the X- and Y-direction, respectively. The X-direction is the positive direction and the Y-direction is the negative direction. We used different mining methods; i.e., we exploited the full thickness of 4 m and the height of 2 m to conduct a comparative study to explore the effect of the pore water pressure in the aquiclude on the periodic sinking of the cover rock and the water inrush. The model is presented in Figure 2. The model exerts self-weight strain and the initial pore water pressure is in the vertical direction based on the actual conditions. The two sides of the model exert a specific gradient horizontal stress in addition to the lateral pressure generated by the self-weight strain to attain a certain horizontal stress [31, 32]. In order to conform to actual mining conditions, the computing begins with the formation of an in situ stress field and a seepage field. The mining exploitation moves into the X-direction in steps. The waterproof coal pillars remain to prevent the water inrush. In the simulation experiment, there are no coal pillars.

3.3. Simulation Results

3.3.1. Spatial-Temporal Characteristics of the Pore Water Pressure with Full Thickness Exploitation. The analysis of the spatial-temporal characteristics of the pore water pressure and roof water inrush is conducted by observing the changes in the pore water pressure of the aquiclude for different distances to the working face. Because the roof water inrush occurs due to the dynamic load effect of the main top, the data of integral multiple of step distance of 20 m of the mine's average periodic weighting are selected. We divided the aquiclude into slices along the levels parallel with the X-face and Y-face, respectively, to observe the changes in the pore water pressure. Image processing was conducted on the data and the results are displayed using three-dimensional water pressure nephograms and contour maps.

It is evident from Figure 3 that the results change with the propulsion distance of the pore water pressure of the aquiclude. When the distance is 20 m from the working face, the goaf is in the first periodic pressure and the pore water pressure of the corresponding aquiclude decreases from 1.59 MPa to 1.44 MPa and the water pressure decreases to 0.15 MPa; therefore, a local subsidence funnel is formed within a certain range. The descending coefficient is only 0.09 and the change is not obvious. This indicates that the pore water pressure of the aquiclude in this location changes with the dynamic load transfer of the mining disturbance; however, the influence of the mining activity on the pore water pressure is limited. When the working face is at a distance of 40 m, the pore water pressure funnel further expands in both the strike and dip directions of the face and its forward subsidence boundary lags behind the position of the working face. The pore water pressure is 1.37 MPa and the minimum value occurs in the deepest spot of the funnel. The water pressure decreases to 0.07 MPa when the distance to the working face is 20 m. The water pressure of the aquiclude is stable. When the distance to the working face is 60 m, "the descending funnel" deepens markedly and the pore water pressure changes suddenly from 1.37 MPa to 0.72 MPa. The descending coefficient is 0.55 relative to the initial water pressure. Simultaneously, the extent of the descending funnel of high pore water pressure increases. It is observed in the contour nephogram that areas with a large hydraulic gradient are generated at a location lagging 22 m behind the two ends of the working face. The fact shows that the water inrush positions are located in the goaf areas behind the two ends of the working face. This change is sudden and hysteretic and a large amount of hydrostatic power is released. This can be described as the "distortion" of the water pressure. Under actual conditions, this type of roof water inrush would cause large damage and endanger people's lives. In order to monitor the changes in the layer's water pressure after the water inrush, the advance distance of the working face is increased to 80 m and the water inrush is not as serious. The conditions are better. The pore water pressure of the aquiclude returns gradually to 1.24 MPa and the two contour lines that converged and were caused by the roof water inrush change into a single funnel. These details indicate that the aquiclude resists the influx of the water to some degree due to the continuous compaction from the overburden load. The pore water pressure increases; however, it does not reach a stable value before the roof water inrush. When the distance to the working face is 100 m, the pore water pressure decreases rapidly to 0.85 MPa. It is observed that when the full thickness of 4 m is mined, a cycle of "destruction-recovery-destruction" occurs in the aquiclude with the successive advance of the working face and

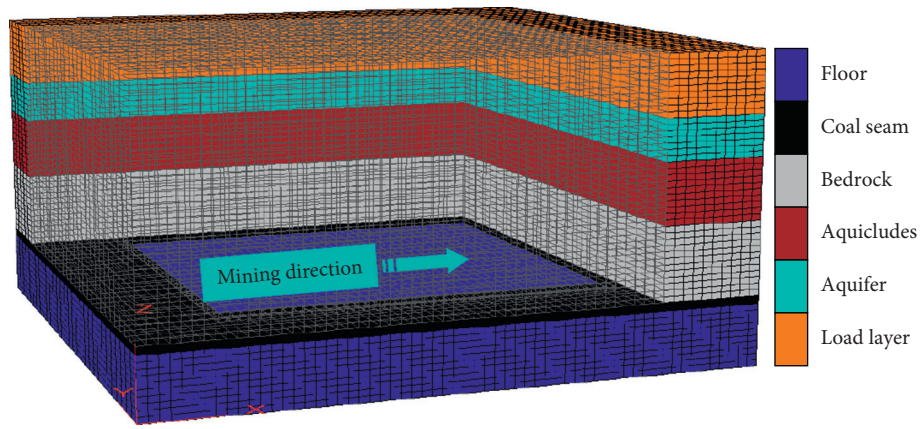

Figure 2: Coupling model.

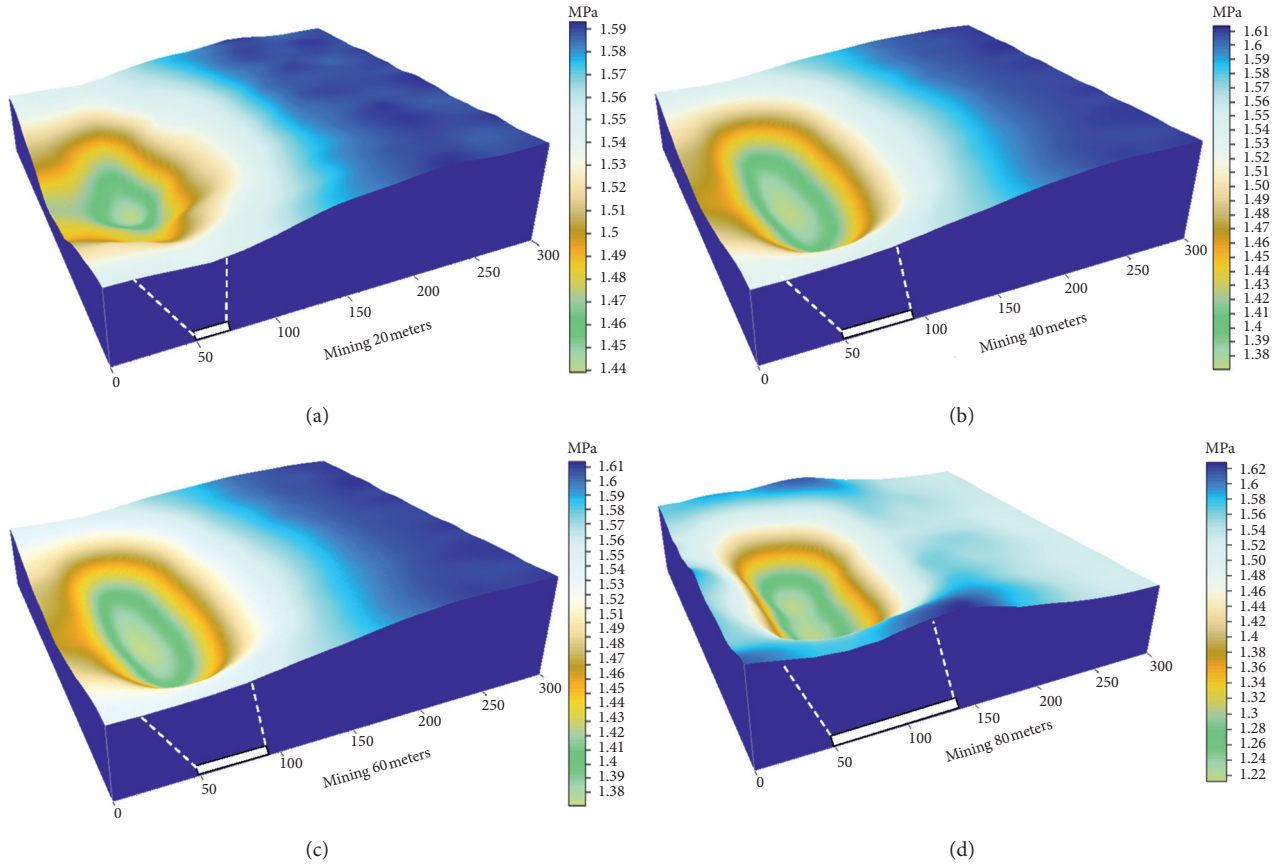

Figure 3: Continued.

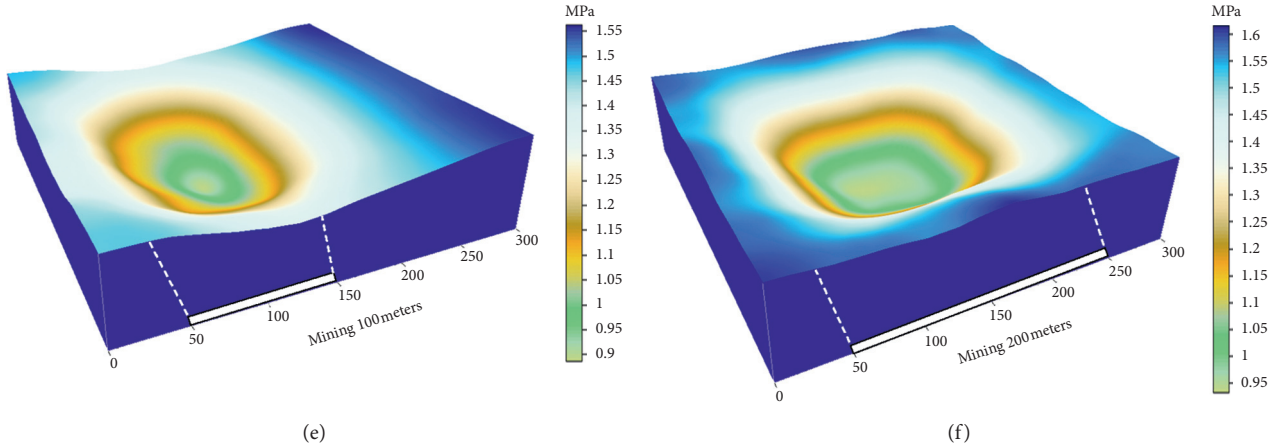

(e) (f)

Figure 3: Response characteristics of the pore water pressure.

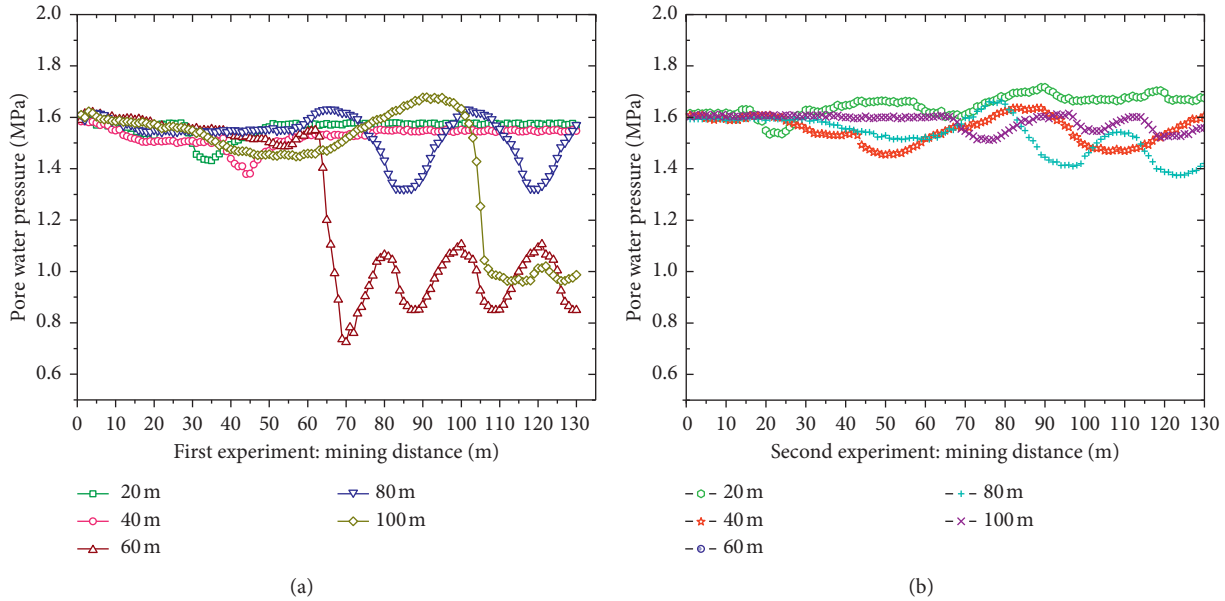

(a) (b)

Figure 4: Graphs of pore water pressure.

the transfer of the periodic load. After several distortions of the periodic pore water pressure of the aquiclude and at a distance to the working face of 200 m, the three-dimensional map of the pore water pressure shows a descending concave surface responding to the underground goaf. The center point of the concave surface along the Z-direction coincides with the geometric center point of the goaf. The minimum pore water pressure is 0.92 MPa and the pore water pressure of the descending concave surface boundary is 1.51 MPa, which is close to the initial pore water pressure.

3.3.2. The Spatial-Temporal Characteristics of the Pore Water Pressure of the Exploitation to the Height of 2 m. In the second experiment, the mining height is 2 m. The period, position, and data selection are the same as in the first experiment to determine the pore distortion under different mining intensities. Figure 4 shows the changes in the pore water pressure of the two experiments.

For the mining of the full thickness of 4 m and at a distance to the working face of 60 m, the pore water pressure of the aquiclude increases rapidly. When the mining position of 60 m is reached, the pore water pressure decreases abruptly. In the subsequent advance process, the pore water pressure fluctuates around the amplitude of 0.32 MPa. The second roof water inrush does not occur until the distance to the working face is 100 m. However, the unloading speed and unloading value are both not up to their equivalents during the first roof water inrush. In the second experiment, the mining height is 2 m. The pore water pressure fluctuates when the distance to the working face is 40 m; no rapid decrease in the pore water pressure is observed and the water pressure fluctuates around the initial water pressure value of 1.59 MPa. The maximum value is 1.71 MPa, the minimum is

1.37 MPa, and the average amplitude is 0.17 MPa. Unlike in the first experiment, in the second experiment, the aquiclude bears the dynamic load in different areas and the stress field and seepage field also change as the periodic roof stress of working face changes based on the changes in the pore water pressure. The pore water pressure changes that correspond to the time point i reflect the roof's periodic stress. In the first experiment, the occurrence of the roof water inrush can be predicted by the sudden distortion of the pore water pressure. In the second design, the small fluctuations are within the safety range. This means that the seepage volume of the mining roof fluctuates within the security threshold.

4. Conclusions

We elucidated the spatial-temporal relationships between the pore water pressure in the aquiclude and the roof water inrush. Based on the analytic solutions, numerical simulations, and analog experiments of the pore water pressure changes in the aquiclude, we draw the following conclusions.

(1) The amplitude of the water pressure of the aquiclude can be obtained in real time by using the analytical formula of the pore water pressure in the soil layer and taking into account the frequency of the applied load caused by the mining activities and the material parameters of the soil layers. Subsequently, the dynamic relationships between the pore water pressure and the advance of the working face can be described; a comparison of the amplitude of the water pressure and the maximum water pressure indicates the threshold causing the water inrush.

(2) Different mining intensities affect the aquiclude to various degrees, leading to changes in the pore water pressure and the roof seepage volume. At a high mining intensity, a distortion funnel with high pore water pressure appears in the roof area of the goaf and the water inrush is most serious at the two ends of the working face. In contrast, when the mining intensity is low, the pore water pressure in the roof area of the goaf fluctuates slightly but does not increase or decrease rapidly.

(3) In this study, we conducted multiple approaches to demonstrate the spatial-temporal characteristics and to provide a theoretical foundation for the development of a roof water inrush forecasting system based on the pore water pressure changes of the soil layer.

Data Availability

All data generated or analyzed during this study are included in this article.

Conflicts of Interest

The authors declare that they have no conflicts of interest regarding the publication of this paper.

Authors' Contributions

T. Y. and J. L. conceived and designed the experiments; L. W. and S. W. analyzed the data; and T. Y. wrote the paper.

Acknowledgments

This study was supported by the National Natural Science Foundation of China (nos. 52004200 and 51774229) and China Postdoctoral Science Foundation (no. 2020M673609XB). The funding by both agencies is gratefully acknowledged.

References

[1] F. Limin, M. Xiongde, L. Yonghong et al., "Geological disasters and control technology in high intensity mining area of western China," *Journal of China Coal Society*, vol. 42, no. 2, pp. 276–285, 2017.

[2] H. Liu, T. Yang, B. Zhang, Y. Li, and X. Hou, "Influence factors of overlying coal strata falling and mine pressure behaviours in western coal mines," *Journal of China Coal Society*, vol. 42, pp. 460–469, 2017.

[3] J. Zhang, T. Yang, Y. Tian, and B. Wang, "Experimental test for destruction law of aquiclude under action of mining and seepage," *Rock and Soil Mechanics*, vol. 36, pp. 219–224, 2015.

[4] M. Qian, "On sustainable coal mining in China," *Journal of China Coal Society*, vol. 35, no. 4, pp. 529–534, 2010.

[5] X. Jia, W. Zhu, and X. Wang, "Study on water-inrush mechanism and prevention during coal mining under unconsolidated confined aquifer," *Journal of Mining and Safety Engineering*, vol. 28, pp. 333–339, 2011.

[6] D. Jin, "New development of water disaster prevention and control technology in China coal mine and consideration on methodology," *Coal Science & Technology*, vol. 45, pp. 141–147, 2017.

[7] L. Fan, M. Xiang, J. Peng et al., "Groundwater response to intensive mining in ecologically fragile area," *Journal of China Coal Society*, vol. 41, pp. 2672–2678, 2016.

[8] J. Zhang and T. Yang, "Study of a roof water inrush prediction model in shallow seam mining based on an analytic hierarchy process using a grey relational analysis method," *Arabian Journal of Geosciences*, vol. 11, no. 7, p. 153, 2018.

[9] F. Cui, Q. Wu, Y. Lin, Y. Zeng, and K. Zhang, "Damage features and formation mechanism of the strong water inrush disaster at the Daxing Co mine, Guangdong Province, China," *Mine Water and the Environment*, vol. 37, no. 2, pp. 346–350, 2018.

[10] J. Wu, S. C. Li, Z. H. Xu, D. D. Pan, and S. J. He, "Flow characteristics after water inrush from the working face in karst tunneling," *Geomechanics and Engineering*, vol. 14, pp. 407–419, 2018.

[11] Y. Zeng, Q. Wu, S. Liu, Y. Zhai, H. Lian, and W. Zhang, "Evaluation of a coal seam roof water inrush: case study in the Wangjialing coal mine, China," *Mine Water and the Environment*, vol. 37, no. 1, pp. 174–184, 2018.

[12] Y. Gao, "Four-zone model of rockmass movement and back analysis of dynamic displacement," *Journal of China Coal Society*, vol. 21, pp. 51–56, 1996.

[13] L. Shi, H. Xin, P. Zhai et al., "Calculating the height of water flowing fracture zone in deep mining," *Journal of China University of Mining and Technology*, vol. 41, pp. 37–41, 2012.

[14] Q. Wu, H. Xu, Y. Zhao, and J. Cui, "Dynamic visualization and prediction for water bursting on coal roof based on "three

maps method"" *Journal of China Coal Society*, vol. 41, pp. 2968–2974, 2016.

[15] L. Fan, X. Ma, H. Jiang, and S. Cheng, "Risk evaluation on water and sand inrush in ecologically fragile coal mine," *Journal of China Coal Society*, vol. 41, pp. 531–536, 2016.

[16] L. Wang and Q. Han, "Application of flooding forecasting system to coal mining under sea," *Coal Geological and Exploration*, vol. 34, pp. 54–56, 2006.

[17] W. Sui and Q. Dong, "Variation of pore water pressure and its precursor significance for quicksand disasters due to mining near unconsolidated formations," *Chinese Journal of Rock Mechanics and Engineering*, vol. 27, pp. 1908–1916, 2008.

[18] T. Yang, C. Tang, Z. Tan, W. Zhu, and Q. Feng, "State of the art of inrush models in rock mass failure and developing trend for prediction and forecast of groundwater inrush," *Chinese Journal of Rock Mechanics and Engineering*, vol. 26, pp. 268–277, 2007.

[19] Q. Huang, B. Wei, and W. Zhang, "Study of downward crack closing of clay aquiclude in shallowly buried coal seam," *Journal of Mining and Safety Engineering*, vol. 27, pp. 35–39, 2010.

[20] Z. Zhang, X. Lu, Y. Chen, B. Chen, and P. Li, "Experimental study on excess pore water pressure of soils covered by clay layer," *Chinese Journal of Rock Mechanics and Engineering*, vol. 22, no. 1, pp. 131–136, 2003.

[21] F. Du, H. Bai, H. Huang, and G. Jiang, "Mechanical analysis of periodic weighting of main roof in longwall top coal caving face with thin bedrock roof," *Journal of China University of Mining and Technology*, vol. 42, pp. 362–369, 2013.

[22] M. A. Biot, "Generalized theory of acoustic propagation in porous dissipative media," *The Journal of the Acoustical Society of America*, vol. 34, no. 9, pp. 1254–1264, 1962.

[23] C. Wei and K. K. Muraleetharan, "Acoustical characterization of fluid-saturated porous media with local heterogeneities: theory and application," *International Journal of Solids and Structures*, vol. 43, no. 5, pp. 982–1008, 2006.

[24] O. C. Zienkiewicz, C. T. Chang, and P. Bettess, "Drained, undrained, consolidating and dynamic behaviour assumptions in soils," *Géotechnique*, vol. 30, no. 4, pp. 385–395, 1980.

[25] G. Bai, "Fluid solid coupling model of equivalent continuous medium in overburden rock based on FLAC^{3D} and its application," *Journal of Mining and Safety Engineering*, vol. 27, pp. 106–110, 2010.

[26] F. Du and K. Wang, "Unstable failure of gas-bearing coal-rock combination bodies: insights from physical experiments and numerical simulations," *Process Safety and Environmental Protection*, vol. 129, pp. 264–279, 2019.

[27] F. Du, K. Wang, X. Zhang, C. Xin, L. Shu, and G. Wang, "Experimental study of coal-gas outburst: insights from coal-rock structure, gas pressure and adsorptivity," *Natural Resources Research*, vol. 29, no. 4, pp. 2481–2493, 2020.

[28] J. Zhang and Z. Hou, "Experimental study on simulation materials for solid-liquid coupling," *Chinese Journal of Rock Mechanics and Engineering*, vol. 23, pp. 3157–3161, 2004.

[29] Q. Liu, J. Chai, S. Chen, D. Zhang, Q. Yuan, and S. Wang, "Monitoring and correction of the stress in an anchor bolt based on pulse pre-pumped brillouin optical time domain analysis," *Energy Science and Engineering*, vol. 8, no. 6, pp. 2011–2023, 2020.

[30] Q. Liu, S. Chen, S. Wang, J. Chai, and D. Zhang, "Experimental development process of a new cement and gypsum-cemented similar material considering the effect of moisture," *Geofluids*, vol. 2020, Article ID 8831801, 14 pages, 2020.

[31] K. Wang and F. Du, "Coal-gas compound dynamic disasters in China: a review," *Process Safety and Environmental Protection*, vol. 133, pp. 1–17, 2020.

[32] C. Xin, F. Du, K. Wang, C. Xu, S. Huang, and J. Shen, "Damage evolution analysis and gas-solid coupling model for coal containing gas," *Geomechanics and Geophysics for Geo-Energy and Geo-Resources*, vol. 7, p. 7, 2021.